JOURNAL OF AIRCRAFT
Vol. 45, No. 4, July–August 2008

Prediction of the Necessary Degrees of Freedom for Helicopter Real-Time Simulation Models

Marilena D. Pavel*
Delft University of Technology, 2629 HS Delft, The Netherlands

DOI: 10.2514/1.34278

The purpose of this paper is to examine the mathematical modeling of the helicopter flight dynamics for simulator qualification and to reveal new insights into the mathematical model's response fidelity. The paper will focus on the qualification process of the simulator mathematical model as given by joint aviation requirement STD-1H, the European standard for helicopter simulator qualification. Using the joint-aviation-requirement tolerances, defined as acceptable differences between the model results, the flight test data, and the critical-pole-distance method developed at Delft University of Technology for predicting the necessary degrees of freedom of a simulation model, the paper will perform a sensitivity study on the pitch tolerances specified by the joint-aviation-requirement regulation, investigating how these tolerances might affect the model level of detail. It will be demonstrated that depending on the rotor system, the tolerances may or may not affect the helicopter flight dynamics behavior. For an articulated centrally hinged rotor, it will be shown that the tolerances have very little effect on the level of detail used in the modeling; for a hingeless rotor, variations in the model from an uncoupled flap-body dynamics to a coupled flap-body result in large variation in the simulation results and handling-qualities characteristics.

Nomenclature

a_1	=	longitudinal disc tilt with regard to no-feathering plane, rad
h	=	distance between the helicopter center of gravity and rotor hub
I_y	=	helicopter moment of inertia around pitch axis, $\text{kg} \cdot \text{m}^2$
K_A, K_H	=	moment exerted on the body per radian of tilt for an articulated and hingeless rotor
K_β	=	flapping hinge spring, Nm/rad
M_{hel}	=	helicopter mass, kg
m_{bl}	=	blade mass, kg
N	=	number of blades
N_1, N_2	=	terms including the uncoupled system characteristics in the critical-pole-distance criterion
q	=	helicopter pitch rate, rad/s
s	=	Laplace variable
$\mathbf{T}_{\text{dp}}$	=	helicopter thrust with regard to the disc plane, N
T_{12}, T_{21}	=	terms including the uncoupled system characteristics in the critical-pole-distance criterion
T'_{12}, T'_{21}	=	negative terms T_{12}, T_{21}
t	=	time variable
$\mathbf{u}$	=	vector of control variables in the linearized equations of motion
$\mathbf{x}$	=	vector of state variables in the linearized equations of motion
x_1, x_2	=	degrees of freedom of a two-degree-of-freedom system
γ	=	Lock number
θ_{1s}	=	longitudinal cyclic, rad
ξ_1, ξ_2	=	damping ratio of the degrees of freedom x_1 and x_2
τ	=	time constant of first-order flapping dynamics
ψ	=	azimuth angle, rad
Ω	=	rotor rotational speed, rad/s
ω_1, ω_2	=	natural frequencies of the x_1 and x_2 degrees of freedom, rad/s

Presented as Paper 6206 at the AIAA Modeling and Simulation Technologies Conference and Exhibit, San Francisco, 15–18 August 2005; received 27 August 2007; accepted for publication 26 December 2007. Copyright © 2008 by Marilena D. Pavel. Published by the American Institute of Aeronautics and Astronautics, Inc., with permission. Copies of this paper may be made for personal or internal use, on condition that the copier pay the $10.00 per-copy fee to the Copyright Clearance Center, Inc., 222 Rosewood Drive, Danvers, MA 01923; include the code 0021-8669/08 $10.00 in correspondence with the CCC.

*Assistant Professor, Research Group of Design, Integration and Operations of Aircraft and Rotorcraft, Faculty of Aerospace Engineering, Kluyverweg 1; m.d.pavel@tudelft.nl. Member AIAA.

I. Introduction

FLIGHT simulators have become indispensable tools for both training and research. In the effort to replicate the actual multitude of flying maneuvers and conditions of the real aircraft, both the simulator mathematical model and the motion and visual systems are becoming increasingly sophisticated. Clearly, developing extensive simulation models (i.e., models including sophisticated kinematics, structural, aerodynamic, and control dynamic aspects) can be useful when one attempts to accurately reproduce the characteristics of the system. Nevertheless, a flight simulator cannot perfectly represent the aircraft in all aspects: the mathematical model of the aircraft is never fully accurate, and the motion and visual systems have physical limitations that make the full representation of the sensation of flying always less than perfect. Also, sophisticated simulator mathematical models are not convenient for use in obtaining physical insight into the mechanism of coupling between the different motion degrees of freedom.

Regulatory authorities have established standards to be used by simulator manufacturers in the process of acceptance and certification of their simulators. For helicopters, the most widely recognized standard for simulation qualification is Federal Aviation Administration advisory circular AC 120-63 [1], which is currently being reworked into joint-aviation-requirement (JAR) STD-1H [2]. These standards provide criteria for both the vehicle's flight dynamics mathematical model and for each of the major components of a helicopter simulator, including the simulator systems (i.e., motion system, image generation system, control loading system, etc.).

In terms of validating current simulator mathematical models, the current experience of simulator manufacturers shows that 80% fidelity can now be achieved with a physical model; the remaining 20% requires artificial tuning. The tuning process represents corrections applied to the physical parameters of the model to improve the correlation between the flight test data and the model. Tuning is done when the tolerances prescribed by JAR (i.e., the differences between the model results and the flight test data) are not attained. However, although tuning can rectify problems in a specific flight condition, it may actually have an adverse effect on other parts

of the flight envelope. Furthermore, tuning is often applied to one component of the system (most often, the vehicle model) to compensate for effects being caused elsewhere (for example, motion gains and washout frequencies). As a result, the modeling modifications may be physically unrealistic and difficult to justify from the standpoint of a flight dynamics engineer. This can result in the simulator failing some of the quantitative tests, and engineering judgment is often required to resolve problems in these situations. Recent work [3] of the Group for Aeronautical Research and Technology in Europe (GARTEUR) Action Group HC-AG12 has highlighted the need for more substantiation of the relationship between the fidelity and the tolerances.

Before commencing the actual derivation of a simulation model, it is therefore important for the designer to have some indication of how much detail should be included in the model in terms of how many degrees of freedom are needed, which significant degrees of freedom are to be included, what couplings are between the degrees of freedom considered (aerodynamic, gyroscopic, Coriolis, structural, etc.), and which of them are relevant. At the Faculty of Aerospace Engineering at Delft University of Technology, a general prediction method called the critical-pole-distance (CPD) method [4] was developed, which can be used by the design analyst to determine the necessary degrees of freedom to be considered in a low-frequency simulation model for rotary-wing devices before actually commencing the derivation of the complete model. The exercise of this paper is mainly to present 1) the application of the critical-pole-distance method for determining the coupling between the rotor disc-tilt motion (often ambiguously called *flapping dynamics* in the literature) and the helicopter body motion and 2) the connection between the level of detail in modeling and the simulator tolerances.

The paper is structured as follows: Section II presents a brief survey on the necessary degrees of freedom for helicopter simulation models. Section III reviews the CPD method as presented in [4] and derives a criterion for coupling between two modes. Section IV analyzes a simple maneuver in a body and a body-flapping model using the CPD method and determines the effect of simulator tolerances on the handling qualities (HQs). Section V discusses conclusions and potential further extension to this work.

II. Brief Survey on the Necessary Degrees of Freedom for Helicopter Simulation Models

For an articulated rotor, a 6-DOF model seems sufficient to determine natural aircraft behavior. However, for a hingeless-rotor helicopter, the classical 6-DOF approximation is usually no longer applicable, even if only natural helicopter behavior (i.e., without the augmentation system) is considered. This is because for an articulated helicopter, the dynamics of the fuselage and rotor can usually be seen as a cascade problem [5] (i.e., a rapid rotor plane response followed by a slower fuselage response), but for hingeless-rotor configurations, the body motion speeds up and the rotor dynamics affect the body dynamics. Therefore, for a hingeless rotor, models including rotor dynamics must usually be used in real-time simulation. Chen et al. [6] presented a review of the research done (during a couple of decades) on the development and validation of flight dynamics models by NASA and the U.S. Army. Their conclusion was that depending on the specific application, the number of degrees of freedom considered in the development of helicopter mathematical models and flight laws for handling-quality purposes vary between a 6-DOF fuselage and quasi-static rotor; 9-DOF fuselage and rotor flap; 10-DOF fuselage, rotor flap, and rpm or fuselage, rotor flap, and rotor lag; and 16-DOF fuselage, rotor flap, rotor lag, pitch, and rpm, with linear and nonlinear aerodynamics. Linear aerodynamics refers to simplifications such as a small angle of flapping and inflow and the use of the simple blade theory with no compressibility or stall effects included. According to Chen et al. [6], simplified linear aerodynamics models may be used for exploratory investigations within the flight envelope: for basic aircraft, a 6-DOF linear model for low-frequency maneuvers and a 9- or 10-DOF model for high-frequency maneuvers, and for stability and control augmentation system research, a 6- or 9-DOF linear aerodynamics model to determine the fuselage feedback and a 9-, 10-, 12-, or 16-DOF linear aerodynamics model to determine the rotor/fuselage feedback. For investigations involving exploration at the edge of the flight envelope, nonlinear aerodynamics effects must be included in the simulations.

III. Critical-Pole-Distance Method

During the design of helicopters, simulation models are developed to predict the helicopter behavior in different conditions. Clearly, developing simulation models for rotary wings is a difficult and time-consuming task. Clearly, the simulation phase is, in general, a time-consuming stage. The models used should be as simple as possible, as far as is consistent with the required accuracy and the specific case considered. The preparation phase when the dynamic equations of motion are derived is especially a very time-consuming effort. The effort needed to derive the equations of motion and the computational effort increase each exponentially, with the number of structural degrees of freedom taken into consideration. The reason for this is that every new degree of freedom added to the model gives rise not only to an additional equation of motion, but also to a large amount of coupling terms in all the other differential equations. Therefore, it is important that before the actual derivation of a simulation model is commenced, there must be some indications of the relevant degrees of freedom and how much detail should be considered in the model. A prediction of the necessary features of the model should take into consideration the required accuracy of the simulation, the kind of loading cases considered, and the purpose for which the simulation results will be used. A general prediction method, the critical-pole-distance method [4], was developed at Delft University of Technology to be used by the design analyst to determine the necessary degrees of freedom to be considered when developing a mathematical model for simulating the helicopter flight dynamics. A number of methods have been developed for determining the necessary degrees of freedom to be considered in the simulation models [7–9]. All these methods first need to derive the equation of motions of the fully coupled system to make further simplifications. The strength of the CPD method is that the designer can obtain some indication of the relevant degrees of freedom and how much detail should be considered in a simulation model *before* actual model derivation is commenced. The method is especially suited for building case-specific models revealing physical insight into phenomena observed in complex systems. The CPD method may be considered to be an extension of the classic Campbell diagram (also named the spoke diagram, Southwell diagram, and fan plot), one of the most important tools for understanding the dynamic behavior of a rotating machine. The benefit of the CPD method relative to the Campbell diagram is that whereas the Campbell diagram gives information only on the system's frequencies, the critical-pole-distance method reveals both the frequencies and the damping existing in the system. For the sake of completeness, next is a review of the CPD method and the principles from which it was derived. The CPD method contains the following steps:

1) First, considering the helicopter as a summation of mutually *uncoupled* subsystems blades, hub, fuselage, etc., the equations of motion for every uncoupled deflection mode are derived.

2) Subsequently, for each subsystem, the formulated equations of motion are solved. The solutions represent the uncoupled mode eigenvalues and can be represented in the complex plane. The eigenvalue representation in the complex plane has the advantage of providing information on structural mode behavior in frequency as well as in damping. The frequency shows whether the mode under consideration is a vibration, and the damping gives information on the damping-type forces (of aerodynamic, gyroscopic, structural, Coriolis, or other nature) involved in the system, which can have a stabilizing effect on the motion.

3) Next, using the representation in the complex plane, critical regions are defined. A critical region is an area of the complex plane in which potential couplings between different modes occur both within and between subsystems. The criterion for a critical region is the relative position of the poles in the complex plane (i.e., if, in the

complex plane, the poles associated with the uncoupled motion of different modes are close together); one may expect that these modes will couple.

4) Finally, conclusions concerning the degrees of freedom to be used in the structural model can be drawn. The modes involved in the structural model will be divided into three classes: modes to be discarded from the model, modes to be kept separately in the model (neglecting the coupling terms between these modes and other degrees of freedom), and modes to be kept in the model (including the coupling effects that are essential for the model).

The crucial question posed by the CPD method was how the relative distance and position of the poles actually correlate with the strength of the intermodal couplings or, in other words, what the interpretation of the relative position and proximity of different poles and/or excitation sources meant. To answer this question, [4] formulated the critical-pole-distance criterion, which could be applied to quantify the relative position of two poles found in close proximity. The criterion depends exclusively on the *uncoupled* frequencies and damping characteristics of the modes involved in the motion. However, its quantification is based on the information given by the full set of *coupled* equations.

A. Critical-Pole-Distance Criterion for a Two-Degree-of-Freedom System

The present section reviews the derivation of the CPD criterion as described in [4]. Consider a two-degree-of-freedom linearly coupled system of equations of motion of a dynamic system in the form:

$$\begin{cases} \ddot{x}_1 + 2\xi_1\omega_1\dot{x}_1 + \omega_1^2 x_1 + f_{12}\ddot{x}_2 + g_{12}\dot{x}_2 + h_{12}x_2 = 0 \\ \ddot{x}_2 + 2\xi_2\omega_2\dot{x}_2 + \omega_2^2 x_2 + f_{21}\ddot{x}_1 + g_{21}\dot{x}_1 + h_{21}x_1 = E(t) \end{cases} \tag{1}$$

where the terms $f_{12}, g_{12}, h_{12}, f_{21}, g_{21}$, and h_{21} represent the coupling terms and $E(t)$ is an external excitation force applied only to the degree of freedom x_2. The present section investigates the conditions under which the degrees of freedom x_1 and x_2 can be assumed to be weakly coupled in the model. In the Laplace domain, the system of equations can be written as

$$\begin{cases} (s^2 + 2\xi_1\omega_1 s + \omega_1^2)\widehat{x}_1(s) + (f_{12}s^2 + g_{12}s + h_{12})\widehat{x}_2(s) = 0 \\ (f_{12}s^2 + g_{21}s + h_{21})\widehat{x}_2(s) + (s^2 + 2\xi_2\omega_2 s + \omega_2^2)\widehat{x}_2(s) = \widehat{E}(s) \end{cases} \tag{2}$$

Introducing the following notations,

$$\begin{aligned} N_1(s) &= \left(s^2 + 2\xi_1\omega_1 s + \omega_1^2\right) \\ T_{12}(s) &= \left(f_{12}s^2 + g_{12}s + h_{12}\right) \\ N_2(s) &= \left(s^2 + 2\xi_2\omega_2 s + \omega_2^2\right) \\ T_{21}(s) &= \left(f_{21}s^2 + g_{21}s + h_{21}\right) \end{aligned} \tag{3}$$

the equations of motion can equivalently be written as

$$\begin{cases} N_1(s)\widehat{x}_1(s) + T_{12}(s)\widehat{x}_2(s) = 0 \\ T_{21}(s)\widehat{x}_1(s) + N_2(s)\widehat{x}_2(s) = \widehat{E}(s) \end{cases} \tag{4}$$

Next, each degree of freedom can be defined as an excitation for the other degree of freedom. In the equations of motion (4), this is equivalent to moving the degrees of freedom involved in the couplings to the right-hand side of the equation and moving the degrees of freedom containing the uncoupled characteristics of the system to the left-hand side. The system of equations (4) can then be expressed as

$$\begin{cases} N_1(s)\widehat{x}_1(s) = T'_{12}(s)\widehat{x}_2(s) \\ N_2(s)\widehat{x}_2(s) = T'_{12}(s)\widehat{x}_1(s) + \widehat{E}(s) \end{cases} \tag{5}$$

where T'_{12} and T'_{21} are the coefficients T_{12} and T_{21} passed to the right-hand side of the equations with a minus sign. The reason for this is that by doing so, the equations of motion can be transformed from an open-loop control system into a closed-loop control system, involving a specific degree of freedom to be investigated in the forward loop and the degrees of freedom that may couple to the degree of freedom analyzed in the backward loop. Note that whereas the uncoupled eigenvalues are contained in the denominator terms N_1 and N_2 of the transfer functions, the coupling terms are contained only in the numerator terms T_{12} and T_{21}. The equations of motion (4) can be treated as block diagrams involving transfer functions in an open-loop control system; Eqs. (5) can be treated as transfer functions in a closed-loop control, defining a transfer function $F(s)$ in the feedforward loop and a transfer function $G(s)$ in the feedback loop as

$$\begin{cases} \frac{\widehat{x}_1}{\widehat{x}_2} = \frac{T'_{12}(s)}{N_1(s)} = G(s) \\ \frac{\widehat{x}_2}{\widehat{x}_1} = \frac{T'_{21}(s)}{N_2(s)} = F(s); \;\; \frac{\widehat{x}_2}{\widehat{E}} = \frac{1}{N_2(s)} = H(s) \end{cases} \tag{6}$$

The equations of motion may be represented as in Fig. 1.

The following relations may be applied to the block diagrams represented in this figure:

$$\begin{cases} \widehat{x}_1(s) = G(s)\widehat{x}_2(s) \\ \widehat{x}_2(s) = F(s)\widehat{x}_1(s) + H(s)\widehat{E}(s) \end{cases} \tag{7}$$

Eliminating $\widehat{x}_1$ in Eq. (7) leads to the following closed-loop transfer function:

$$\frac{\widehat{x}_2(s)}{\widehat{E}(s)} = \frac{H(s)}{1 - F(s)G(s)} \tag{8}$$

Returning to the initial question of the present section of whether the degrees of freedom x_1 and x_2 are weakly coupled or not, this question is equivalent to that of whether the closed-loop transfer function

$$\frac{\widehat{x}_2(s)}{\widehat{E}(s)}$$

differs from

$$\left(\frac{\widehat{x}_2(s)}{\widehat{E}(s)}\right)_0$$

where the index zero indicates that the feedback $G = 0$. Substituting this in Eq. (8) leads to

$$G(s) = 0 \Rightarrow T'_{12} = 0 \Rightarrow \left(\frac{\widehat{x}_2(s)}{\widehat{E}(s)}\right)_0 = H(s) \tag{9}$$

Thus, the degrees of freedom x_2 and x_1 are weakly coupled when the relative difference between the transfer function of the coupled system

$$\frac{\widehat{x}_2(s)}{\widehat{E}(s)}$$

and that the uncoupled system

$$\left(\frac{\widehat{x}_2(s)}{\widehat{E}(s)}\right)_0$$

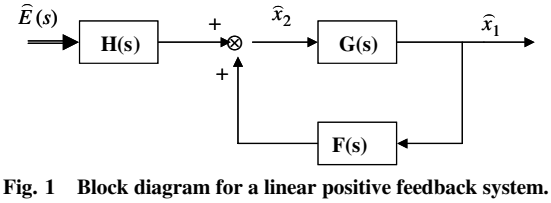

Fig. 1 Block diagram for a linear positive feedback system.

is approximately zero in any point s of the complex plane; that is,

$$\left[\frac{\widehat{x_2}(s)}{\widehat{E}(s)} - \left(\frac{\widehat{x_2}(s)}{\widehat{E}(s)}\right)_0\right] \Big/ \left(\frac{\widehat{x_2}(s)}{\widehat{E}(s)}\right)_0 = \frac{F(s) - G(s)}{1 - F(s)G(s)}$$
$$= \frac{1}{N_1(s)N_2(s)/T'_{12}(s)T'_{21}(s) - 1} \cong 0 \tag{10}$$

Equation (10) gives the condition of weak (loose) coupling between the degrees of freedom x_2 and x_1 in a two-degree-of-freedom linear coupled system. This condition is fulfilled when

$$\frac{N_1(s)N_2(s)}{T'_{12}(s)T'_{21}(s)} \to \infty$$

that is, when either $N_1(s)N_2(s) \to \infty$ (if $T'_{12}(s)T'_{21}(s) \neq \infty$) or $T'_{12}(s)T'_{21}(s) \to 0$ (if $N_1(s)N_2(s) \neq 0$). Equivalently, this means

$$T'_{12}(s)T'_{21}(s) \ll N_1(s)N_2(s) \tag{11}$$

or when

$$N_1(s)N_2(s) \ll T'_{12}(s)T'_{21}(s) \tag{12}$$

Condition (11) states that the two degrees of freedom x_1 and x_2 are weakly coupled when the product of their coupled characteristics is small with respect to that of the uncoupled characteristics. Equivalently, condition (12) states that if the product containing the uncoupled characteristics is sufficiently large compared with that containing the coupled characteristics, then the degrees of freedom x_1 and x_2 may also be considered to be weakly coupled. Condition (11) is quite often referred to in literature and requires the investigation of the couplings in the system. Condition (12) refers to the uncoupled characteristics of the system and contains the information to be investigated in the critical-pole-distance criterion. One may observe that conditions (11) and (12) may be applied only to certain classes of problems. Indeed, the limit

$$\frac{T'_{12}(s)T'_{21}(s)}{N_1(s)N_2(s)} \to 0$$

cannot be determined in the extreme cases of 0/0 (zero cross-coupling and zero characteristics) and ∞/∞ (very large cross-coupling and system characteristics). In addition, the cases $0/\infty \to 0$, $\infty/0 \to \infty$, and $x/0 \to \infty$ should not be investigated because these are not relevant for the designer (for example, in the case of zero cross-coupling, one is not interested in how large the product of the uncoupled characteristics is because the two degrees of freedom will not interfere with each other anyway). The class of problems that is relevant to criterion (10) is that for which the system is not on the edge of its operating envelope and the coupling and uncoupling terms are in the same order.

Because s is the Laplace operator and thus a generally complex variable, $s = a + ib$, it follows that $N_1(s)$, $N_2(s)$, $T'_{12}(s)$, and $T'_{21}(s)$ are also complex variables. Using the representation of the complex numbers in the complex plane by their radius and argument, it can be demonstrated that conditions (11) and (12) may be satisfied if and only if their modulus satisfies the same conditions as well:

$$|T'_{12}(s)T'_{21}(s)| \to 0 \Rightarrow |T'_{12}T'_{21}| \ll |N_1N_2| \tag{13}$$

or

$$|N_1(s)N_2(s)| \to \infty \Rightarrow |N_1N_2| \gg |T'_{12}T'_{21}| \tag{14}$$

Condition (14) demonstrates that a criterion in the critical-pole-distance method may be derived from this condition and used as an engineering approach in the preparation phase of simulation models (when the couplings in the system are unknown) to determine how much detail should be used in the model. Returning to Eq. (3) and putting $N_1(s) = 0$ and $N_2(s) = 0$, the system poles are obtained (assuming an oscillatory motion for the system):

$$s_{12} = -\xi_1\omega_1 \pm i\omega_1\sqrt{1 - \xi_1^2}, \qquad s_{34} = -\xi_2\omega_2 \pm i\omega_2\sqrt{1 - \xi_2^2} \tag{15}$$

Substituting $s = a + ib$ in its general form as a complex variable into Eq. (3) and calculating the product $|N_1N_2|$ of the uncoupled degrees of freedom, one obtains

$$|N_1N_2| = \sqrt{[(a^2 - b^2) + \omega_1(\omega_1 + 2a\xi_1)]^2 + 4b^2(a + \xi_1\omega_1)^2}$$
$$\cdot \sqrt{[(a^2 - b^2) + \omega_2(\omega_2 + 2a\xi_2)]^2 + 4b^2(a + \xi_2\omega_2)^2} \tag{16}$$

which is a function that depends on the coordinates of the complex variables a and b and on the system characteristics ξ_1, ω_1, ξ_2, and ω_2. Condition (14) states that the product $|N_1N_2|$ has to be much larger than the product of the coupling terms $|T'_{12}T'_{21}|$ to be able to neglect the couplings in the system. This condition should be investigated in every point in the complex plane $s \in C$, except the points s_{12} and s_{34}, where $|N_1N_2|$ is always zero and the condition can never be fulfilled.

The question is what the critical values for s are that can reveal valuable information to the designer on the system characteristics as defined by the frequency, damping, and coupling terms. One should, in this context, realize that a value s far away from the region of the poles of the system will always lead to a very large value of the product $|N_1N_2|$ and that the information on the system characteristics in damping and frequencies will be lost. Therefore, such points do not contribute to the understanding of the quantification of the product $|N_1N_2|$, unless the couplings are also investigated.

On the other hand, assuming s is in the region of the poles s_{12} and s_{34}, the designer can obtain useful information about the system characteristics by analyzing condition (13). A large value for the product $|N_1N_2|$ in this region will show that the system poles are situated sufficiently far from each other to neglect the couplings in the systems (assuming the case of nonzero couplings $|T'_{12}T'_{21}| = 0$).

On the basis of the preceding discussion and considering a point $s \to \xi_1\omega_1 + i\omega_1$ (note that this point is not the pole of the motion and that it is taken only at the coordinate of the undamped frequency of the degree of freedom x_1) and recalling Eq. (16), condition (14) will become

$$|N_1N_2| = \xi_1\omega_1\sqrt{\left(9\xi_1^2\omega_1^2 + 16\omega_1^2\right)}\left\{\left[\xi_1^4\omega_1^4 + 2\xi_1^2\omega_1^2\left(\omega_1^2 + 2\xi_2^2\omega_2^2\right)\right.\right.$$
$$\left.\left. + 4\xi_1\omega_1\xi_2\omega_2\left(\omega_1^2 + \xi_1^2\omega_1^2 + \omega_2^2\right) + 4\xi_1\omega_1\xi_2\omega_2\left(\omega_2^2 - \omega_1^2\right)^2\right]\right\}^{1/2}$$
$$\gg |T'_{12}(\xi_1 i\omega_1) \cdot T'_{21}(\xi_1 i\omega_1)| \tag{17}$$

Condition (17) requires the determination of the coupling terms, which, incidentally, are not known before developing a complete coupled model. However, this condition includes the *necessary condition* to consider two degrees of freedom as weakly coupled; that is,

$$|N_1N_2| = \xi_1\omega_1\sqrt{\left(9\xi_1^2\omega_1^2 + 16\omega_1^2\right)} \cdot \sqrt{\left[\xi_1^4\omega_1^4 + 2\xi_1^2\omega_1^2\left(\omega_1^2 + 2\xi_2^2\omega_2^2 + \omega_2^2\right) + 4\xi_1\omega_1\xi_2\omega_2\left(\omega_1^2 + \xi_1^2\omega_1^2 + \omega_2^2\right) + 4\xi_1\omega_1\xi_2\omega_2\left(\omega_2^2 - \omega_1^2\right)^2\right]} \text{ is large} \tag{18}$$

Condition (18) is considered as a criterion in the critical-pole-distance method to investigate the critical regions of couplings. This condition is a necessary condition, but, in general, it is not sufficient. There are applications in which this condition is also sufficient (such an application, for example, may be a system that is only coupled through stiffness and in which the inertial couplings are absent). Of course, the interpretation of the term large is subjective and has to be defined for a certain dynamic system, a specified unit of measure, and a certain class of problems. Note that the frequencies ω_1 and ω_2, are nondimensionalized by means of the rotor rotational velocity Ω to transform the value for $|N_1N_2|$ into a nondimensional value. Returning to the initial restrictions under which condition (18) was derived, it should be remembered that this condition cannot be applied to a system with zero-cross couplings. In such systems, it does not matter how large the quantity $|N_1N_2|$ is, the system is always uncoupled. Reference [4] derived the critical-pole-distance criterion (18) for the particular case of the poles close to the imaginary axis.

1. Poles Situated Near the Imaginary Axis

When the poles of the motion are near the imaginary axis, the critical region is close to the imaginary axis and thus one may assume that s is a purely imaginary value: $s = ib$. The product $|N_1N_2|$ as given by Eq. (16) can then be calculated as $(omega_1^2 - b^2)^2 * (omega_2^2 - b^2)^2$

$$|N_1N_2| = \sqrt{\left(\omega_1^2 - b^2\right)^2\left(\omega_2^2 - b^2\right)^2 + 16\xi_1^2\xi_2^2\omega_1^2\omega_2^2b^4 + 4\xi_1^2\omega_1^2b^2\left(\omega_2^2 - b^2\right)^2 + 4\xi_2^2\omega_2^2b^2\left(\omega_1^2 - b^2\right)^2} \tag{19}$$

Choosing s close to the pole of the degree of freedom x_1 ($s \to i\omega_1$) to obtain information mainly on the system's uncoupled characteristics, condition (18) in the critical-pole-distance criterion becomes

$$|N_1N_2| = \sqrt{16\xi_1^2\xi_2^2\omega_1^6\omega_2^2 + 4\xi_1^2\omega_1^2\left(\omega_2^2 - \omega_1^2\right)^2} \tag{20}$$

Condition (20) may be considered to be the critical-pole-distance criterion for two poles situated near the imaginary axis. Observe that condition (20) may be satisfied if either the difference between the uncoupled natural frequencies of the degrees of freedom x_1 and x_2 is sufficiently large,

$$\left(\omega_2^2 - \omega_1^2\right)^2 \tag{21}$$

or, in case the uncoupled frequencies are almost equal ($\omega_1 \cong \omega_2$), if the product of the damping ratios is large, then

$$\xi_1^2\xi_2^2 \tag{22}$$

is large.

In other words, two degrees of freedom with poles situated near the imaginary axis may be considered to be weakly coupled if their uncoupled eigenvalues are either sufficiently separated in frequency or both are sufficiently damped. According to Eq. (22), which refers to the product of damping ratios, both modes need to be sufficiently damped to be considered to be weakly coupled (or, in other words, it is not sufficient for only one mode to be well damped; if the other mode is not sufficiently damped, the two modes remain coupled). This conclusion corresponds to the ground-resonance analysis of helicopters, in which Deutsch [10] derived a criterion to avoid ground-resonance phenomena based on the product of the blade and hub damping, which is more significant than the damping in the blades and the hub individually. The designer is thus left with the choice of how to distribute the damping between two modes as long as their product in damping adds up to a certain value.

2. Poles Situated Near the Real Axis

When the poles of the motion are near the real axis, the critical region is close to the real axis and one may assume s as a real value: $s = a$. The product $|N_1N_2|$ as given by Eq. (16) can then be calculated as

$$|N_1N_2| = \sqrt{a^4 + a^2\left(\omega_1^2 + \omega_2^2\right)^2 + 2a^3(\omega_1\xi_1 + \omega_2\xi_2) + \omega_1\omega_2(\omega_1 + 2a\xi_1) + (\omega_2 + 2a\xi_2)} \tag{23}$$

Choosing s close to the pole of the degree of freedom x_2 ($s \to -\xi_2\omega_2$), condition (18) in the critical-pole-distance criterion becomes

$$|N_1N_2| = \sqrt{\omega_2^4\xi_2^4 + \omega_2^2\xi_2^2\left(\omega_1^2 + \omega_2^2\right) + \omega_1\omega_2\left(\omega_1\omega_2 + 4\xi_1\xi_2^3\omega_2^2\right) - 2\xi_1^3\omega_2^3(\xi_1\omega_1 + \xi_2\omega_2) - 2\omega_1\omega_2^2\xi_2(\xi_1 + \xi_2)} \tag{24}$$

Criterion (24) may be considered as the critical-pole-distance criterion of two poles of motion situated near the real axis.

B. Generalization of the Critical-Pole-Distance Criterion

Reference [4] generalized the CPD criterion for an n-degree-of-freedom system of the form

$$\begin{cases} \ddot{x}_1 + 2\xi_1\omega_1\dot{x}_1 + \omega_1^2x_1 + f_{12}\ddot{x}_2 + g_{12}\dot{x}_2 + h_{12}x_2 + \cdots + f_{1n}\ddot{x}_n + g_{1n}\dot{x}_n + h_{1n}x_n = 0 \\ f_{21}\ddot{x}_1 + g_{21}\dot{x}_1 + h_{21}x_1 + \ddot{x}_2 + 2\xi_2\omega_2\dot{x}_2 + \omega_2^2x_2 + \cdots + f_{2n}\ddot{x}_n + g_{2n}\dot{x}_n + h_{2n}x_n = 0 \\ \cdots \\ \ddot{x}_j + 2\xi_j\omega_j\dot{x}_j + \omega_j^2x_j + \cdots + f_{jn}\ddot{x}_n + g_{jn}\dot{x}_n + h_{jn}x_n = E(t) \\ \cdots \\ f_{n1}\ddot{x}_1 + g_{n1}\dot{x}_1 + h_{n1}x_1 + \cdots + \ddot{x}_n + 2\xi_n\omega_n\dot{x}_n + \omega_n^2x_n = 0 \end{cases} \tag{25}$$

where the terms $f_{12}, \ldots, f_{n,n-1}$, $g_{12}, \ldots, g_{n,n-1}$, and $h_{12}, \ldots, h_{n,n-1}$ represent the coupling terms, and $E(t)$ is an external excitation force applied only to the degree of freedom x_j. Applying the Laplace transformation to the system of equations (25) and assuming each degree of freedom as an excitation for the remaining $n - 1$ degrees of freedom, after applying a sudden input ε to the system $\widehat{E}(s) = \varepsilon T_\varepsilon(s)$, the system of equations (25)

can be equivalently written as

$$\begin{bmatrix} N_1\hat{x}_1 & & & & \\ & N_2\hat{x}_2 & & & 0 \\ & & N_i\hat{x}_i & & \\ 0 & & & N_j\hat{x}_j & \\ & & & & N_n\hat{x}_n \end{bmatrix} + \begin{bmatrix} 0 & T_{12} & & & T_{1n} \\ T_{21} & 0 & & & T_{2n} \\ \cdots & & & & \\ T_{i1} & T_{i2} & 0 & & T_{in} \\ \cdots & & & & \\ T_{j1} & T_{j2} & & 0 & T_{jn} \\ \cdots & & & & \\ T_{n1} & T_{n2} & & & 0 \end{bmatrix} \begin{Bmatrix} \hat{x}_1 \\ \hat{x}_2 \\ \cdots \\ \hat{x}_i \\ \cdots \\ \hat{x}_j \\ \cdots \\ \hat{x}_n \end{Bmatrix} = \varepsilon \begin{Bmatrix} 0 \\ 0 \\ \cdots \\ 0 \\ \cdots \\ T_\varepsilon \\ \cdots \\ 0 \end{Bmatrix} \tag{26}$$

where

$$N_k = s^2 + 2\xi_k\omega_k s + \omega_k^2 s$$
$$T_{kl} = f_{kl}s^2 + g_{kl}s + h_{kl} \quad \text{with} \quad k = 1 \ldots n, \quad l = 1 \ldots n, \quad k \neq 1 \tag{27}$$

Following the same reasoning as in the case of a two-degree-of-freedom system, [4] demonstrated that the degree of freedom x_j decouples from the remaining $n-1$ degrees of freedom of system (25) when, in any point of the complex plane, the relative difference between the transfer function of the coupled system $(\hat{x}_j/\varepsilon)$ and the transfer function of the system with the degree of freedom x_j weakly coupled $(\hat{x}_j/\varepsilon)_0$ is approximately zero; that is,

$$\frac{(\hat{x}_j/\varepsilon)-(\hat{x}_j/\varepsilon)_0}{(\hat{x}_j/\varepsilon)_0} = \frac{N_j\Delta_{jj}^*}{\Delta} = \frac{1}{(-1)^{j+1}(T_{j1}/N_j)(\Delta_{j1}^*/\Delta_{jj}^*)+\cdots+(-1)^{j+n}(T_{jn}/N_j)(\Delta_{jn}^*/\Delta_{jj}^*)} - 1 \cong 0 \tag{28}$$

implies that x_j decouples from $x_1, \ldots, x_n$, where $\Delta_{j1}^*, \ldots, \Delta_{jn}^*\phi$ are the minors of the elements $T_{j1}, \ldots, T_{jn}$ and are the determinants obtained by deleting the line j and, respectively, the columns 1 to n in Δ:

$$\Delta_{j1}^* = \begin{vmatrix} T_{12} & T_{1n} \\ \cdots & \\ T_{j-1,2} & T_{j-1,n} \\ T_{j+1,2} & T_{j+1,n} \\ \cdots & \\ T_{n1} & N_n \end{vmatrix}, \qquad \Delta_{jn}^* = \begin{vmatrix} N_1 & T_{1n-1} \\ \cdots & \\ T_{j-1,1} & T_{j-1,n-1} \\ T_{j+1,1} & T_{j+1,n-1} \\ \cdots & \\ T_{n1} & T_{n,n-1} \end{vmatrix} \tag{29}$$

Observe that in the generalized case, the critical-pole-distance criterion (28) contains both the uncoupled and the coupled terms of the investigated degree of freedom x_j. For example, in a three-degree-of-freedom system, assuming that the input ε is applied to x_2, the critical-pole-distance criterion (28) becomes

$$\frac{(\hat{x}_j/\varepsilon)-(\hat{x}_j/\varepsilon)_0}{(\hat{x}_j/\varepsilon)_0} = \left[\left(\frac{T'_{32}T'_{23}}{N_2N_3} + \frac{T'_{12}T'_{21}}{N_1N_2} - \frac{T'_{12}T'_{23}T'_{31}}{N_1N_2N_3} - \frac{T'_{32}T'_{21}T'_{13}}{N_1N_2N_3}\right) \Big/ \left(1 - \frac{T'_{32}T'_{23}}{N_2N_3} - \frac{T'_{12}T'_{21}}{N_1N_2} + \frac{T'_{12}T'_{23}T'_{31}}{N_1N_2N_3} + \frac{T'_{32}T'_{21}T'_{13}}{N_1N_2N_3}\right)\right] \cong 0 \tag{30}$$

which implies that x_2 decouples from x_1 and x_3, where $T'_{12}, T'_{13}, \ldots, T'_{32}$ are the coefficients $T_{12}, T_{13}, \ldots, T_{32}$ passed to the right-hand side of Eqs. (26) with a minus sign. Concluding, in an $n \geq 3$-degree-of-freedom linearly coupled system, determining whether *one* degree of freedom decouples from *all* the other degrees of freedom requires the computing of the coupling terms in the critical-pole-distance criterion. However, the critical-pole-distance method only involves the analysis of those poles situated in critical regions of the complex plane. Poles situated in such regions signify that the corresponding modes of motion are potentially coupling. It follows that although n degrees of freedom are involved, in the critical-pole-distance method, one is primarily interested in the degrees of freedom corresponding to critical regions in the complex plane defined on the basis of the relative position of the poles. In these regions, one has to decide whether poles are sufficiently separated or whether they are sufficiently close to allow for their coupling effects in the model. The critical-pole-distance criterion should therefore not be applied to all couplings between one degree of freedom and the remaining degrees of freedom of the system, but to specific couplings as identified by the critical regions.

IV. Effects of Rotor Disc-Tilt Dynamics on Helicopter Real-Time Simulation Models

A. Simple Maneuver Flown Without Flapping Dynamics

To get some insight into the coupling between the body motion and the disc-tilt motion of the rotor, a simple helicopter maneuver will be investigated. Consider, as an example, the first few instants during the transition from hover to forward flight after a step input of longitudinal cyclic pitch. One may assume that at the very beginning of this maneuver, before forward speed builds up and becomes important, the helicopter just rotates in the pitch direction, as seen in Fig. 2.

The equation of motion describing the helicopter pitch in the shaft plane is

$$-T_{\text{dp}}h(\theta_{1s} - a_1) - \frac{N}{2}K_\beta(\theta_{1s} - a_1) = I_y\dot{q} \Leftrightarrow \dot{q} = -K(\theta_{1s} - a_1) \tag{31}$$

where

$$K = \frac{\mathbf{T}_{\text{dp}}h + (N/2)K_\beta}{I_y}$$

is the moment exerted on the body per radian of rotor disc tilt due to the thrust vector $\mathbf{T}_{\text{dp}}$ offset with regard to the center of gravity $\mathbf{T}_{\text{dp}} = M_{\text{hel}}g$, as well as due to the direct spring moments of constant K_β; N is the number of blades; I_y is the helicopter moment of inertia; h is the distance to the rotor hub; θ_{1s} is the longitudinal tilt of the swashplate; a_1 is the longitudinal disc tilt; and q is the pitching velocity of the body.

In the classical treatment of the subject, the rotor disc tilt is often assumed to respond instantaneously to the pitching motion:

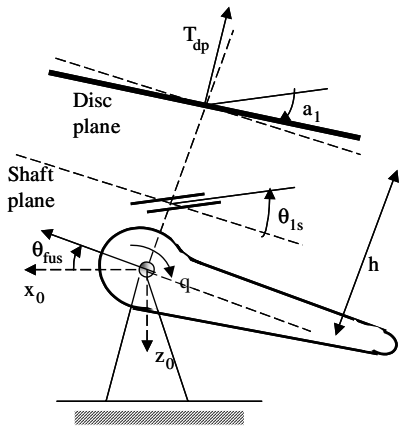

Fig. 2 Helicopter pitch motion after a step input of longitudinal cyclic.

$$a_1 = -\frac{16}{\gamma}\frac{q}{\Omega} \tag{32}$$

where γ is the Lock number and Ω is the rotor angular speed. Equation (32) includes the flapping motion through the steady-state longitudinal rotor disc tilt a_1, neglecting the transient disc-tilt dynamics. This assumption is generally true because the transient disc-tilt indeed damps out very quickly after a disturbance. Together, Eqs. (31) and (32) represent the equations of motion for a pitching helicopter as usually represented in the 6-DOF model (i.e., disc-tilt motion included in a steady-state form).

It can be demonstrated that when trying to simulate the helicopter maneuvering in the pitch axis, a large diversity in helicopter responses is obtained, depending on the particular helicopter rotor system. Consider next the following numerical example (midsized helicopter): mass $M_{\text{hel}} = 2200$ kg, rotor speed $\Omega = 260$ rpm, rotor distance to body center of gravity $h = 1$ m, moment of inertia $I_y = 10,625$ kg $\cdot$ m^2, Lock number $\gamma = 6$, number of blades $N = 3$, and a rotor system of 1) zero stiffness $K_\beta \approx 0$ Nm/rad, representing a centrally hinged rotor system and 2) a large stiffness $K_\beta \approx 460,000$ Nm/rad, representing a hingeless rotor. Assume that the blade is hinged at the hub. Next, apply a step input $\theta_{1s} = -1$ deg at $t = 0$ s in the longitudinal cyclic of the helicopter represented by Eqs. (31) and (32). The helicopter pitch response is given in Fig. 3.

From Fig. 3, one can see that there is a big difference in behavior between a hingeless and an articulated-rotor helicopter. Although the articulated helicopter shows a response typical for acceleration control (i.e., the pilot has to control $\dot{q}$ to fly the maneuver and the helicopter is very sensitive at every pilot input), the hingeless case is more characteristic for velocity control, with the response reaching a constant value of pitch rate already within 1 s. The latter system requires much less anticipation from the pilot.

The preceding conclusion (i.e., that the helicopter response depends on the rotor characteristics) can be reinforced by studying the HQs criteria as given by [11]. Consider, for example, the attitude-quickness criterion (see [11], pp. 78) measuring the helicopter's capability to achieve rapid and precise attitude changes when performing sharp pitch maneuvers. Sending a series of $\theta_{1s} = -1$ deg pulses to the longitudinal cyclic of a model represented by Eqs. (31) and (32) and varying the pulse duration from 1 to 5 s, for every pulse, one can calculate the attitude-quickness parameter Q_θ from [11] as the ratio of the maximum pitch rate q_{pk} to the peak attitude angle change $\Delta\theta_{\text{pk}}$; that is,

$$Q_\theta \overset{\text{def}}{=} \frac{q_{\text{pk}}}{\Delta\theta_{\text{pk}}} \ \text{s}^{-1} \tag{33}$$

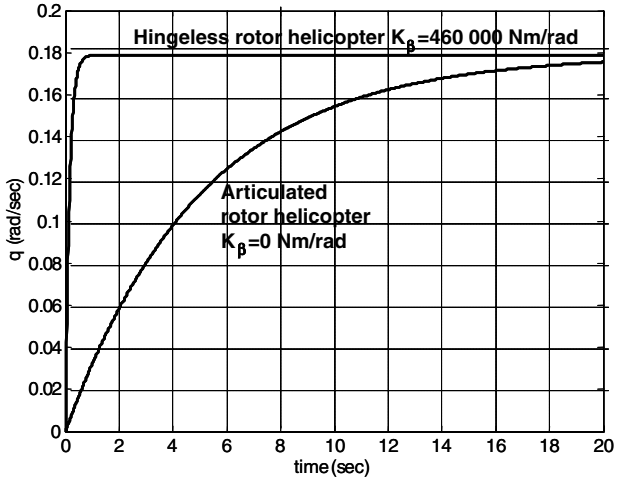

Fig. 3 Pitch response of a hingeless and articulated centrally hinged rotor helicopter.

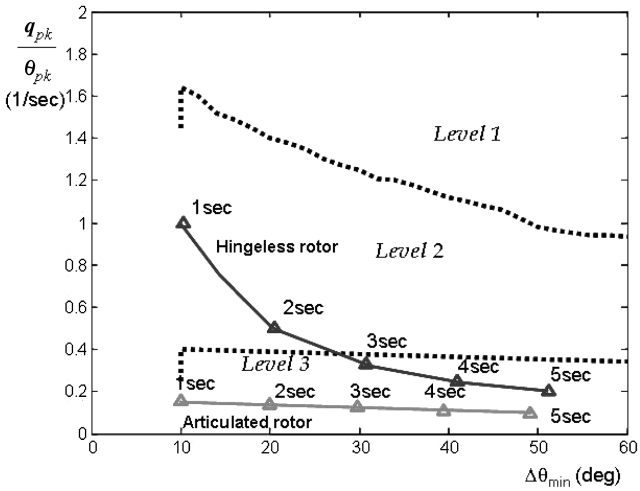

Fig. 4 Attitude-quickness charts for pulses applied to a hingeless and an articulated rotor.

Reference [11] defines handling-quality boundaries for the attitude-quickness parameter as a function of the minimum attitude change $\Delta\theta_{\text{min}}$. Figure 4 presents the attitude-quickness charts for the pulses flown with the articulated and hingeless system on the levels 1–3 boundaries in [11] for a target acquisition and tracking mission. Looking at this figure, one can see that for the hingeless rotor, the HQs deteriorate from level 2 to level 3 as the pulse duration is increasing, whereas for the articulated rotor, the HQs are always in level 3, indicating that the pilot has more difficulty controlling the pitch maneuver.

Next, the effect that the simulator tolerances (as prescribed by JAR-STD) may have on the pilot's perception of reality and, finally, on the simulator credibility will be investigated. One of the most common tests prescribed by JAR to check the simulator fidelity refers to responses to step control inputs performed in the pitch, roll, or yaw axes. For a step maneuver in the pitch axis, JAR prescribes the following acceptable tolerances for the maneuver parameters: in pitch rate, $\pm 10\%$ or ± 2 deg/s and in pitch attitude, $\pm 10\%$ or ± 1.5 deg. The paper will concentrate on the consistency of the [11] pilot performance metrics as measured in the simulator in the pitch axis. It should be pointed out that although the pitch-attitude tolerance as defined by JAR is mainly for the steady-state performance that affects pilot visual cuing in simulator environment, the current analysis is limited in addressing this. Consider that the initial step input of $\theta_{1s} = -1$ deg is flown with the articulated rotor, then implement the maximum upper ($+10\%$) and lower (-10%) deviations in the pitch rate in the model, as given by JAR-STD boundaries.

Next, rewrite the helicopter dynamics in the classical linearized form:

$$\dot{x}(t) = A\mathbf{x}(t) + B\mathbf{u}(t) \tag{34}$$

where $\mathbf{x}$ represents the vector of state variables, $\mathbf{u}$ represents the vector of control variables, A represents the state matrix of stability derivatives, and B represents the control matrix of control derivatives. For Eqs. (31) and (32) giving the helicopter pitch response, this results in

$$\dot{q} = -K\frac{16}{\gamma}\frac{1}{\Omega}q - K\theta_{1s} \Rightarrow A = -K\frac{16}{\gamma}\frac{1}{\Omega}, \qquad B = -K \tag{35}$$

Consider next that the same step input is flown now by varying the system parameters A and B such that the response reaches the JAR boundaries in minimum and maximum allowed deviations. In this way, one can determine the maximum possible variation of parameters A and B (for an n-DOF system, this means matrices A and B) that can be considered in the model satisfying the JAR standard. Parameter A (representing the derivative of pitch moment with regard to pitch rate M_q) and parameter B (representing the derivative

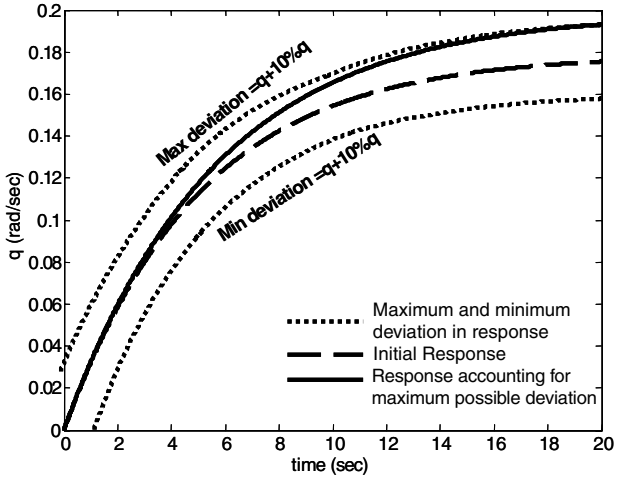

Fig. 5 Pitch response of an articulated rotor simulated with a modified model accounting for the maximum allowed JAR boundary.

of pitch moment with regard to longitudinal cyclic) also vary with the model detail. These derivatives encapsulate a variety of unmodeled moments on the helicopter components. Figure 5 represents the pitch response when parameter A was varied to reach the maximum JAR boundary. For A, a maximum variation between $1.1A$ and $0.9A$ gives the border for minimum-maximum JAR deviation; for B, this variation is between $0.9B$ and $1.1B$. Observe that increasing parameter A results in a deviation to the minimum JAR border, whereas increasing parameter B results in a deviation to the maximum JAR border.

Using the preceding approach, one can determine the effect that the unmodeled parameters may have on the pilot handling qualities (whereas the simulator mathematical model respects the JAR tolerances). For example, consider again the attitude-quickness criterion, this time flying the same series of pulses when varying the A parameter between the minimum and maximum JAR boundaries. Recent work [3] of GARTEUR Action Group AC-AG12 demonstrated that in some cases, considering the aircraft response ranging across the tolerances can give quite different HQ characteristics. Figure 6 plots the attitude quickness for the hingeless and articulated rotors when the A parameter was varied between $1.1A$ and $0.9A$ of the nominal value to reach the allowed JAR boundaries.

Looking at this figure, one can see that increasing the pulse duration results in an increase in the possible variation in quickness. For the hingeless rotor, going from the minimum to the maximum JAR limit results in a slight increase in quickness. For the articulated rotor, the opposite is true. However, although the figure shows a slight variation in quickness as one modifies the model, the HQ level

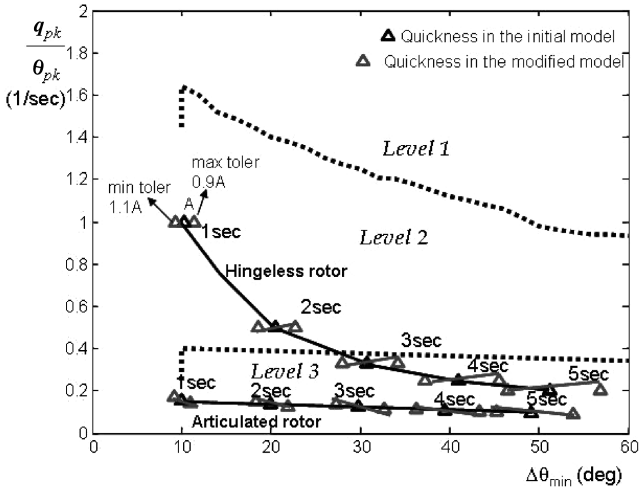

Fig. 6 Attitude-quickness criterion when varying the model parameter A between the upper and lower JAR limits.

remains unchanged: levels 2 and 3 for a hingeless rotor and level 3 for an articulated rotor.

It is also interesting to represent the equivalence between the time domain and the complex domain. Considering the same input in the longitudinal cyclic $\theta_{1s} = -1$ deg and applying the Laplace transformation to the system equations (31) and (32) with zero initial conditions leads to the transfer function:

$$G_{\text{bo}}(s) = \frac{\hat{q}_{\text{bo}}(s)}{\hat{\theta}_{1s}(s)} = \frac{-K}{s + K(16/\gamma)(1/\Omega)} = \frac{1}{(\gamma\Omega/16K)s + 1} \tag{36}$$

The pitch response of the helicopter for a step input $\theta_{1s} = -1$ deg ($\hat{\theta}_{1s} = -1/s$) is then $\hat{q}_{\text{bo}}(s) = G_{\text{bo}}(s)\hat{\theta}_{1s}(s)$. The helicopter motion as given by Eq. (36) may be represented in the complex plane for both the articulated and the hingeless helicopter. The system has one real eigenvalue (pole), which includes the influence of the rotor system via the K value (which depends on K_β):

$$s^A_{\text{bo}} = -K_A \frac{16}{\gamma\Omega}, \qquad s^H_{\text{bo}} = -K_H \frac{16}{\gamma\Omega} \tag{37}$$

Implementing the simulator tolerances in the system motion by varying parameter A (observe that parameter A is equivalent to system poles) results in a movement of helicopter poles, as seen in Fig. 7. Looking at this figure, one can conclude the following:

1) The poles of both the articulated and the hingeless helicopters are situated in the left-hand half of the complex plane and therefore the motion is stable.

2) The closer the pole is to the origin, the slower the motion becomes. Accordingly, the articulated rotor will respond much slower to the longitudinal cyclic than the hingeless rotor, a conclusion confirmed by the time domain representation of Fig. 3. This conclusion can also be verified by calculating the body time constants $\tau^A_{\text{bo}} = (\gamma/16)(\Omega/K_A)$ and $\tau^H_{\text{bo}} = (\gamma/16)(\Omega/K_H)$, which give the articulated rotor the time constant $\tau^{\text{A}}_{\text{bo}} = 5.044$ s and give the hingeless rotor $\tau^H_{\text{bo}} = 0.153$ s. Thus, the articulated rotor is much slower that the hingeless rotor (or, equivalently, the hingeless rotor is much faster than the articulated rotor).

3) Including the tolerances moves the poles of both the articulated and the hingeless helicopters to the left when the minimum tolerance is achieved (which is equivalent to speeding up the helicopter response) and to the right when the maximum tolerance is achieved (which is equivalent to slowing down the response).

B. Effects of Flapping Dynamics on Maneuver Simulation

Consider the same simple maneuver previously investigated (the first few instants of transition from hover to forward flight) and assume now that some dynamics are included in the tilting in the rotor disc in the form of a time constant τ added to Eq. (32):

$$\tau\dot{a}_1 + a_1 = -\frac{16}{\gamma}\frac{q}{\Omega} \tag{38}$$

Reference [4] demonstrated that this kind of extension corresponds to taking into account the low-frequency regressing flapping mode on top of the steady solution. Flying the step input in the longitudinal

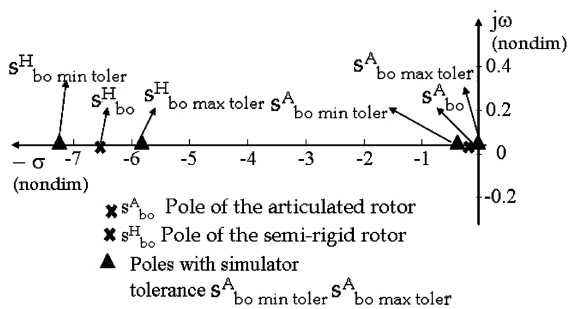

Fig. 7 Poles of the body motion and their migration with simulator tolerances.

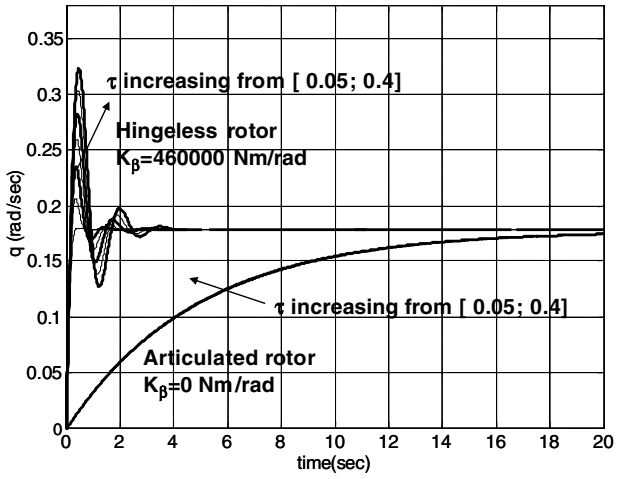

Fig. 8 Influence of flapping dynamics on pitch response.

cyclic of $\theta_{1s} = -1$ deg with Eqs. (31) and (38) and varying the time constant of the first-order flapping dynamics τ from 0.05 to 0.4 gives the helicopter response, as plotted in Fig. 8.

Looking at this figure, it is obvious that although the addition of first-order flapping dynamics does influence the response of the hingeless system, for the articulated system, the addition of flapping dynamics is hardly noticeable. To investigate how noticeable the flapping dynamics are to the pilot, attitude-quickness charts will be plotted when flying different pulse maneuvers of 1–5-s duration. Figure 9 presents attitude-quickness charts for an articulated and hingeless-rotor system when the flapping dynamics were included in the model by varying the flapping time constant τ from 0.05 to 0.4.

Looking at this figure, one can see that indeed, the flapping dynamics influence the attitude-quickness of a hingeless helicopter rather profoundly, the value of attitude-quickness doubling almost as the flapping time constant changes from 0.05 to 0.4. This results in an improvement of the HQs from levels 2 and 3 to level 2. However, for the articulated helicopter, the addition of the flapping dynamics to the model does not change the helicopter HQs.

Next, consider the effect of simulator tolerances added to the body-flapping model and their effect on the helicopter response. Equations (31) and (38) rewritten in matrix form become

$$\begin{Bmatrix} \dot{q} \\ \dot{a}_1 \end{Bmatrix} = \begin{bmatrix} 0 & K \\ -\frac{16}{\gamma}\frac{1}{\Omega\tau} & -\frac{1}{\tau} \end{bmatrix} \begin{Bmatrix} q \\ a_1 \end{Bmatrix} + \begin{Bmatrix} -K \\ 0 \end{Bmatrix} \theta_{1s} \tag{39}$$

Varying the parameters of matrix A and B so that the response reaches the JAR boundaries, one can determine the influence of tolerances (and thus of the unmodeled parameters) on the HQs. The following model variations were found within the JAR boundaries: $A(1,1)$ (i.e., the derivative of pitch moment with regard to the pitch rate) can vary between -0.6 and $+0.7$ for the hingeless rotor with $\tau = 0.05$ and between -0.35 and $+0.35$ for the hingeless rotor with $\tau = 0.4$; for the articulated rotor, a variation -0.05 to $+0.05$ results in attaining the JAR borders regardless of the value of τ. For $A(1,2)$, representing the derivative of the pitch moment with regard to the longitudinal disc tilt, a variation of $1.1A(1,2)$ to $0.9A(1,2)$ was found for a hingeless rotor with $\tau = 0.05$, and a variation of $1.05A(1,2)$ to $0.96A(1,2)$ was found for a hingeless rotor with $\tau = 0.4$; for an articulated rotor, a variation of $1.3A(1,2)$ to $0.8A(1,2)$ was enough to attain the JAR boundaries in pitch response. The preceding variations in model parameters were plotted in the attitude-quickness charts to determine the effects of including the tolerances and thus the level of detail on handling qualities. Figure 10 plots attitude-quickness charts for the hingeless and articulated rotor when the $A(1,2)$ parameter was maximally varied to reach the JAR boundaries and the flapping dynamics were taken into account.

Comparing Fig. 10 with Fig. 6, one can see that including the tolerances in a body-flapping model of a hingeless rotor gives the impression of a light improvement in the HQs. For the articulated rotor, the tolerances included in the body-flapping model give a large change in the pitch attitude achieved in the maneuver.

Consider next the representation in the complex plane of the helicopter motion. Combining Eqs. (31) and (38) and applying the Laplace transformation, the transfer function representing the motion of the helicopter in this case becomes

$$G_{\text{bo-fl}}(s) = \frac{\hat{q}_{\text{bo-fl}}(s)}{\hat{\theta}_{1s}(s)} = \frac{-K(\tau s + 1)}{s(\tau s + 1) + K(16/\gamma)(1/\Omega)} \tag{40}$$

The helicopter pitch response to a step input $\theta_{1s} = -1$ deg ($\hat{\theta}_{1s} = -1/s$) becomes, in this case,

$$\hat{q}_{\text{bo-fl}}(s) = \frac{K(\tau s + 1)}{s(s(\tau s + 1) + K(16/\gamma\Omega))}$$

The poles of the body/disc-tilt motion as given by Eq. (40) are either real or complex values, depending on the sign of the term $1 - 4\tau K(16/\gamma\Omega)$. For the numerical examples considered, the articulated rotor has real poles, whereas the hingeless rotor has complex poles:

$$\begin{aligned} s^A_{\text{bo-fl}} &= -\frac{1}{2\tau} \pm \frac{\sqrt{1 - 4\tau K_A(16/\gamma\Omega)}}{2\tau} \in R \\ s^H_{\text{bo-fl}} &= -\frac{1}{2\tau} \pm i\frac{\sqrt{4\tau K_H(16/\gamma\Omega) - 1}}{2\tau} \in C \end{aligned} \tag{41}$$

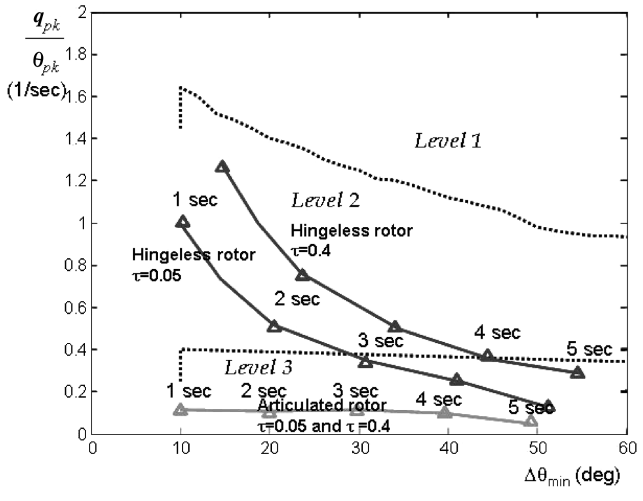

Fig. 9 Attitude-quickness charts for pulses flown in a body-flapping model.

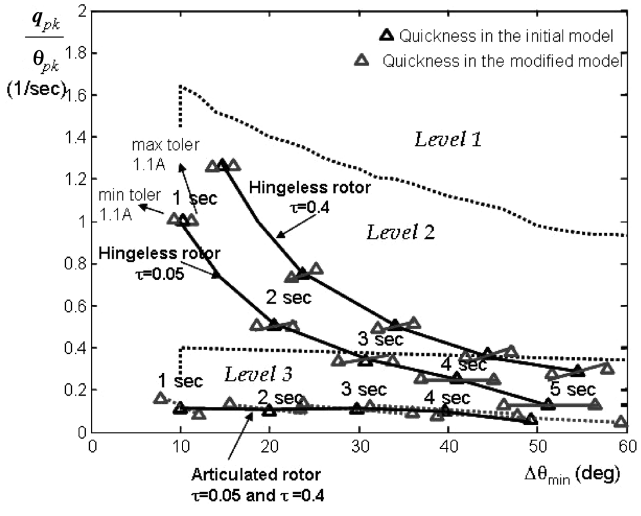

Fig. 10 Attitude-quickness charts including the variation in tolerances on the body-flapping model.

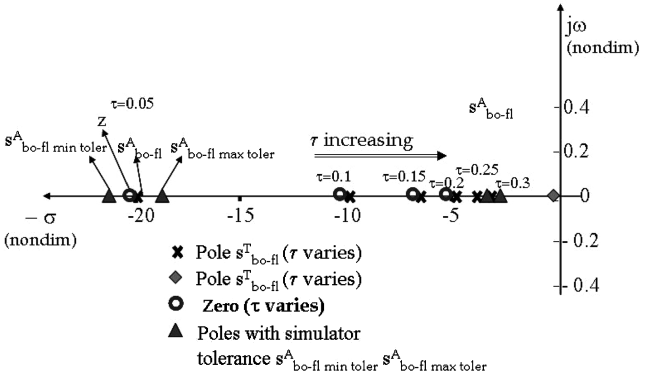

Fig. 11 Coupled body/disc-tilt motion for an articulated rotor.

From Eq. (40), one may observe that adding rotor disc-tilt dynamics to the simulation model introduces a zero in the system $z = -(1/\tau)$. Figures 11 and 12 present the pole-zero pattern of the coupled body/disc-tilt motion as obtained for the articulated and the hingeless rotor when the flapping time constants are varied and the tolerances are added to the model.

For the articulated rotor (see Fig. 11), the motion has two real poles: one pole very close to the origin, which corresponds mainly to the body motion, and another pole far away from the origin, which corresponds mainly to the disc-tilt motion. By increasing the time constant τ, the far pole moves rapidly toward the origin. Because the poles are real and distinct, the motion is a sum of two decaying exponentials. For each pole, a time constant may be defined that is of the form $-1/s^A_{bo-fl}$. Calculating these two time constants for different τ values, it appears that the articulated rotor is characterized by a large time constant corresponding to the pole close to the origin and a smaller one corresponding to the pole far away from the origin. The pole close to the origin is the dominant one, the body motion being mainly determined by this pole. Looking at Fig. 11, one can see that as the disc-tilt time constant increases (the disc-tilt motion slows down), the flap-body pole approaches the body-flapping pole, increasing its influence on the general motion. Concerning the zeros, it is known that they can affect closed-loop stability and performance and trigger instabilities at high gain [12]. If a zero is far away from a pole, it does not influence the transient motion, and therefore it can be neglected, whereas a zero situated close to a pole neutralizes the effect of that pole on the motion. For the articulated rotor, the pole is situated very close to the fast pole (flap-body pole), and therefore it eliminates the effect of the disc-tilt motion on the total pitch motion. Introducing the tolerances in the system slightly changes the pole position, speeding up or slowing the helicopter motion.

For the hingeless rotor, the pole-zero pattern of the coupled body/disc-tilt motion (see Fig. 12) shows that the poles are complex values representing an oscillatory motion. The motion is stable, because the poles are situated in the left-hand side of the complex plane. As the time constant τ increases (disc-tilt motion gets slower), the poles approach the origin, thus increasing the response overshoot and deteriorating the relative stability characteristics of the motion. A time constant of the body/disc-tilt motion may be defined as $1/\varsigma\omega_n = 2\tau$. The body/disc-tilt time constant is reduced (i.e., the speed of decay of the response is increased) by reducing the time constant of the disc-tilt motion (i.e., speeding up the disc-tilt motion), which also results in increasing the real part of the poles (damping) and improving the stability characteristics. The system's response speed is increased by increasing the distance of the poles to the origin (in this case, by increasing K). Therefore, compared with the articulated rotor, the motion speeds up for the hingeless rotor. Concerning the zeros' position, as the zeros approach the origin, the response overshoot is increasing (negative effect), whereas the peak time is decreasing (positive effect). For the hingeless rotor, one may observe that as the disc-tilt time constant increases, the poles approach the origin (i.e., the disc-tilt motion slows down). Introducing the tolerances in the system moves the pole positions up and down (thus increasing and decreasing the eigenfrequency while keeping the damping at the same value). It follows that for the hingeless rotor, the level of detail in the model greatly affects the dynamic helicopter response.

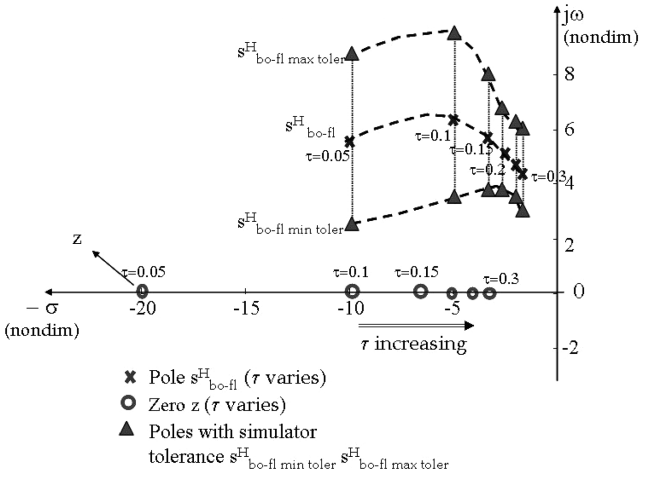

Fig. 12 Coupled body/disc-tilt motion for a hingeless rotor.

C. CPD Method Applied to the Simple Maneuver and Its Relation to Simulator Tolerances

Consider next the CPD method applied to the simple maneuver previously analyzed. This is done to see whether it would be possible for the designer to predict the effect of the disc-tilt dynamics on the body motion before having the coupled body/disc-tilt equations of motion developed. To apply the CPD method to the maneuver, one has to determine the uncoupled body and disc-tilt motion characteristics. The poles of the uncoupled pitch motion are as given in Fig. 7. The poles of the uncoupled disc-tilt motion may be simply determined by calculating the eigenvalue of the uncoupled disc-tilt equation of motion $\tau\dot{a}_1 + a_1 = 0$:

$$s_{\text{fl}} = -1/\tau \tag{42}$$

Observe that increasing the flapping time constant τ moves the s_{fl} pole to the right, thus slowing down the disc-tilt motion. Now the CPD method can be applied. Figures 13 and 14 present the relative position of the uncoupled body and disc-tilt poles for an articulated and a hingeless rotor.

For the articulated rotor, it is obvious that for any value of τ, the body and disc-tilt eigenvalues are relatively far from each other, and therefore the rotor disc-tilt dynamics do not influence the pitch dynamics. Even adding the simulator tolerances does not change the motion characteristics. For the hingeless rotor, as the uncoupled disc-tilt motion slows down (time constant τ increases), it interacts with the region of the uncoupled body pole. For a time constant $\tau \geq 0.1$ s, the body and rotor disc-tilt motion couple together. This result agrees with the conclusions obtained in the time domain and with the HQ investigations. Essentially, for a hingeless rotor, the disc-tilt motion

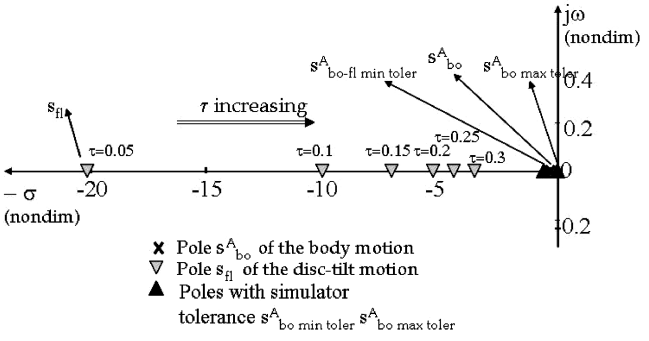

Fig. 13 CPD method applied to an articulated rotor.

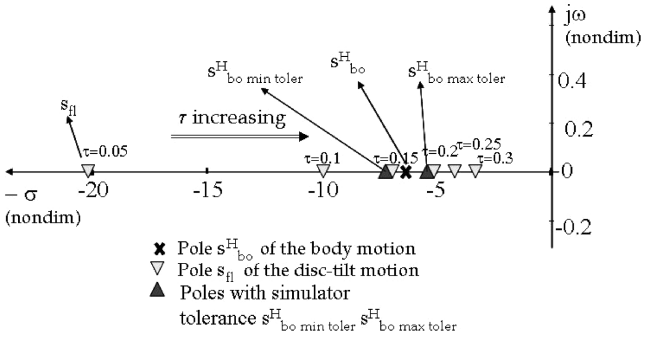

Fig. 14 CPD method applied to a hingeless rotor.

slows down and the body motion speeds up, thus coupling with each other. This is the fundamental explanation of the body/disc-tilt coupling characteristic of hingeless rotors. Introducing simulator tolerances may result in a strengthening of the body-flapping coupling.

V. Conclusions

The goal of the present work was to analyze the effects that the simulator tolerances may have on the level of detail used in the mathematical model. The paper described the critical-pole-distance method, which can be used to predetermine the necessary degrees of freedom required in piloted simulation modeling. This method is actually a formalization of the intuitive fact that in the complex plane representation, regions of agglomeration of eigenvalues represent critical regions in which the corresponding modes couple (in the time domain, this would mean that their time constants are comparable). Specific to this method is that the critical regions are determined by the uncoupled modes of motion, but its criterion is actually an engineering approach to the coupled problem. The main advantage of this method is that the designer can obtain some indication in advance as to the level of model detail required *before* starting to derive the large system of equations of motion that are characteristic to rotary-wing problems. The paper concentrated on the couplings between the body and the rotor disc-tilt motion (flapping motion) in the case of a simple maneuver (i.e., the first few instants during the helicopter transition from hover to forward flight). The CPD method can be applied to more complex cases (for example, simulation models including fuselage, rotor flap, rotor lead lag, pitch, inflow dynamics, etc.); in this case, the CPD criterion must be considered in its general formulation and therefore the coupling terms between the degrees of freedom belonging to identified critical regions must be determined. It was concluded that although the addition of the low-frequency flapping dynamics did influence the response of the hingeless system rather profoundly in such a way that it will probably be noticeable to the pilot, in the case of the articulated system, additional flapping dynamics were hardly noticeable. Introducing the JAR tolerances in the simulation model and assessing the handling qualities of an articulated and a hingeless rotor showed that whereas tolerances may introduce large errors in assessing the HQ characteristics of a hingeless rotor, in the case of an articulated rotor, these tolerances hardly affect the simulation results. Therefore, the tolerances are highly sensitive to the nature of the rotor system used and on the level of detail included in the simulation model. Applying the CPD method to predict the body-flapping coupling showed that, essentially, for a hingeless rotor, the disc-tilt motion slows down and the body motion speeds up, thus coupling these motions. Introducing the simulator tolerances to represent the contribution of other unmodeled system parameters may strengthen or weaken the body-flapping coupling and results in a false pilot interpretation of the handling qualities in the simulator when compared with the real aircraft.

References

[1] "Helicopter Simulator Qualification," Federal Aviation Administration, Advisory Circular FAA AC 120-63, 1994.

[2] "Helicopter Flight Simulators," Joint Aviation Authorities, Standard JAR STD 1H, Hoofddorp, The Netherlands, 2001.

[3] Padfield, G. D., Pavel, M., Casolaro, D., Roth, G., Hamers, M., and Taghizad, A., "Fidelity of Helicopter Real-Time Simulation Models," *61st Annual Forum of the American Helicopter Society*, AHS Internaitonal, Alexandria, VA, June 2005.

[4] Pavel, M. D., "On the Necessary Degrees of Freedom for Helicopter and Wind Turbine Low-Frequency Mode-Modelling," Ph.D. Dissertation, Delft Univ. of Technology, Delft, The Netherlands, Mar. 2001, pp. 59–85.

[5] Curtiss, H. C., Jr., "Stability and Control Modelling," *12th European Rotorcraft Forum*, National Aerospace Lab., Amsterdam, 22–25 Sept. 1986, p. 41.

[6] Chen, R. T. N., Lebacqz, J. V., Aiken, E. W., and Tischler, M. B., "Helicopter Mathematical Models and Control Law Development for Handling Qualities Research," NASA CP-2496, Mar. 1987.

[7] Milne, R. D., "A Method for Improving the Inherent Stability and Control Characteristics of Helicopters," *International Journal of Control*, Vol. 2, No. 2, Feb. 1965, pp. 171–199. doi:10.1080/00207176508905535

[8] Pass, H. B., Pearce, B. F., and Wolkovitch, J., "Topics on Flexible Airplane Dynamics, Part 3: Coupling of the Rigid and Elastic Degrees of Freedom of an Airframe," Systems Technology, Inc., Rept. ASD TDR-63-334, Inglewood, CA, July 1963.

[9] Bielawa, R. L., "*Rotary Wing Structural Dynamics and Aeroelasticity*," 1st ed., AIAA, Washington D.C., 1992, pp. 270–274.

[10] Deutsch, M. L., "Ground Vibrations of Helicopters," *Journal of the Aeronautical Sciences*, Vol. 13, No. 5, May 1946, pp. 223–228.

[11] "Performance Specification, Handling Qualities Requirements for Military Rotorcraft," U.S. Army, Aviation and Missile Command, Aeronautical Design Standard 33E-PRF, Redstone, AL, 21 Mar. 2000.

[12] Lovera, M., Colaneri, P., and Celi, R., "On the Role of Zeros in Rotorcraft Aerodynamics," *Journal of the American Helicopter Society*, Vol. 49, No. 3, July 2004, pp. 318–327.